Available online at www.sciencedirect.com
ScienceDirect
Journal of the European Ceramic Society 32 (2012) 485–494
www.elsevier.com/locate/jeurceramsoc

High temperature oxidation of SiC under helium with low-pressure oxygen. Part 3: β-SiC–SiC/PyC/SiC

K. Dawi [a], M. Balat-Pichelin [a,*], L. Charpentier [a], F. Audubert [b]

[a] *PROMES-CNRS, 7 rue du four solaire, 66120 Font-Romeu – Odeillo, France*
[b] *CEA, DEN, DEC/SPUA/LTEC, 13108 St Paul lez Durance, France*

Received 22 April 2011; received in revised form 26 July 2011; accepted 6 August 2011
Available online 12 October 2011

Abstract

In the frame of generation IV gas-cooled fast reactor (GFR), the cladding materials currently considered is a SiC/SiC-based composite with a pyrocarbon interphase and a β-SiC coating on the surface to close the porosity (noted β-SiC–SiC/PyC/SiC). These elements are subjected to temperatures going from 1300 to 1500 K in nominal operating conditions to 1900–2300 K in accidental conditions. The coolant gas considered is helium pressurized at 7 MPa.

After a thermodynamic study carried out on the oxidation of β-SiC under helium and low oxygen partial pressures, an experimental approach was made on β-SiC–SiC/PyC/SiC composites under active oxidation conditions ($1400 \leq T \leq 2300$ K; $0.2 \leq pO_2 \leq 2$ Pa). This study follows two preceding studies carried out on two polytypes of SiC: α (Part 1) and β (Part 2) under the same conditions. In these studies, the influence of the crystalline structure on the transition temperature between passive and active oxidation and on the mass loss rate was discussed.

The experimental study allows to determine the oxidation rates in incidental and accidental conditions under $pO_2 = 0.2$ and 2 Pa. The variation of the mass loss rates according to the temperature for β-SiC–SiC/PyC/SiC oxidized under $pO_2 = 0.2$ and 2 Pa shows the existence of three domains in the zone of active oxidation. These tests also show the weak impact of the oxygen partial pressure on the mass loss rate of the material in this range of pressure for temperatures lower than 2070 K. On the other hand, beyond 2070 K, an increase of the mass loss rate leading to important damage of the material has been observed, at lower temperature under $pO_2 = 0.2$ Pa than under $pO_2 = 2$ Pa. This variation was associated to the effect of the oxygen partial pressure on the sublimation temperature of SiC. Similar experiments were performed on pre-oxidized samples and on the face without CVD β-SiC coating and both the results are close to the ones obtained for the face with the CVD β-SiC layer.

Keywords: B. Composites; B. Surfaces; C. Corrosion; C. Oxidation; D. SiC; E. Nuclear applications

1. Introduction

The study of the behavior of a new fuel cladding material for the future Gas-cooled Fast Reactor (GFR) is necessary, not only in nominal operating conditions, but also in the case of incident or accident. SiC/PyC/SiC composites covered by a β-SiC coating to close the porosity are the principal structural materials candidate for the cladding of future GFR due to their good mechanical properties at high temperature and their resistance to irradiation.[1] The chemical stability and especially the oxidation resistance of the cladding is one of the important properties for cladding materials since the helium coolant gas can contain a low residual oxygen partial pressure.

The notation of the composites in the following paragraphs is labeled as coating-fiber/interphase/matrix as for example β-SiC–SiC/PyC/SiC for a composite with β-SiC as coating, SiC as fibers and matrix and with a pyrocarbon (PyC) interphase.

Several studies were carried out on the oxidation of composites like SiC–C/SiC, composite C/SiC with a SiC coating and SiC/SiC at high temperature.[2–10] The interesting part of this study lies in the fact that it is carried out at very low oxygen partial pressure ($0.2 \leq pO_2 \leq 2$ Pa) that can be found in the GFR.

The main problem of the current SiC-based composite is the presence of a pyrocarbone interphase (PyC). Under oxidizing atmosphere, this interphase is consumed, for example, according to the following reactions:

$$C(s) + O_2(g) = CO_2(g)$$

$$2C(s) + O_2(g) = 2CO(g)$$

* Corresponding author. Tel.: +33 468 307 768; fax: +33 468 302 940.
E-mail address: marianne.balat@promes.cnrs.fr (M. Balat-Pichelin).

0955-2219/$ – see front matter © 2011 Elsevier Ltd. All rights reserved.
doi:10.1016/j.jeurceramsoc.2011.08.005

In the case of thin interphase (<0.1 μm), the vacuum thus created can be filled with silica, fragile and adherent. A study on the behavior and oxidation mechanism of the SiC/PyC or ML/SiC composites with conventional pyrocarbone interphase (PyC) or advanced multi-layer interphase (ML = *n* PyC–SiC) using thermogravimetric analysis (TGA) under He–O_2 atmosphere at 1270 and 1470 K was carried out recently.[2] It was noted that the SiC/PyC/SiC oxidized at 1470 K and SiC/ML/SiC oxidized at 1270 and 1470 K both present a relatively low mass change during oxidation, associated to relatively fast silica formation on the SiC matrix and fibers, closing the access of oxidizing species before the beginning of the carbon combustion. On the other hand, in the case of SiC/PyC/SiC oxidized at 1270 K, significant mass loss rate was measured, associated with slow silica formation for closing the porosity and avoiding a PyC recession.

The oxidation of SiC/SiC at high temperature has also a great influence on the mechanical properties of the composite. Indeed, in the study of Wu et al.[5] carried out using TGA on the oxidation behavior of SiC–SiC/PyC/SiC composites with 3D Hi-Nicalon fibers, PyC interphase and SiC coating under a mixture Ar/O_2 (78/22 vol.%), three-point bending flexural tests were performed before and after each oxidation experimental test. It was noted that, for temperatures below 1370 K, the composite flexural strength is controlled by the consumption of the PyC interphase, and the oxidation has a small effect on the composite resistance. Beyond 1470 K, the flexural strength in this case is controlled by the degradation of the Hi-Nicalon fibers resistance. In addition, since oxidation takes place throughout the interphase between fibers and matrix, the displacement of the fracture (flexural tests) increases with the increase of the mass loss rate, and the mode of fracture shows non-brittle pattern. This study shows also the relation between the thermal expansion coefficients (CTE) of various components of the composite and the appearance of cracking after oxidation. Indeed, fine microscopic cracks are observed in the matrix of SiC/SiC after oxidation at high temperature. The authors explain these cracks by the difference of CTE between coating and composite and between fibers and matrix.

Other mechanical studies on SiC/SiC composites under oxidizing atmosphere at high temperature were published by Ochiai et al. in air[6] and vacuum.[7] It was shown that the resistance of the SiC/SiC composites decreases with the increase of temperature and experiment duration under vacuum or air, however, the mode of rupture is different in both cases. This degradation of the composites was attributed to the reduction of fibers resistance in the two environments. A simple model was introduced to describe the variation of the composites resistance according to temperature and duration.

The SiC coating can protect the composite from oxidation under air at high temperature by limiting the degradation of the pyrocarbone interphase, hence reducing the mass loss of material. This coating is more efficient at high temperature as we remain within the domain of passive oxidation. The presence of cracks in the coating allows the penetration of oxygen, thus the consumption of the interphase at low temperature.[9] The silica which is formed on the coating at high temperature makes possible to fill in the cracks and to limit the diffusion of oxygen in this case.

This study focuses on the oxidation behavior of β-SiC–SiC/PyC/SiC composite with β-SiC coating at high temperature (1400–2300 K) in helium atmosphere with reduced oxygen partial pressure (0.2 and 2 Pa). This study follows two preceding studies carried out on two polytypes of SiC: α and β under the same conditions[10,11] where the influence of the crystalline structure on the passive/active transition temperature and on the mass loss rate was discussed. In this work, we study the oxidation behavior of β-SiC–SiC/PyC/SiC in a temperature range of nominal operation conditions and in the case of incident or accident for GFR. The mass loss kinetics under accidental operating conditions, the behavior and the lifetime of the cladding were discussed. Various techniques of analysis (SEM, XRD, etc.) coupled to thermodynamic calculations by GEMINI code[12] were used to interpret the results.

2. Thermodynamic study

For the GFR, the SiC/SiC cladding elements are subjected to temperatures ranging from 1300 K in nominal operating conditions to 2300 K in the case of an accident. Thermodynamic calculations were carried out on a wider range of temperatures from 1000 to 2500 K by step of 100 K. The total pressure P^t is fixed at 1 atm (10^5 Pa). The range of oxygen partial pressures studied goes from 0.2 to 100 Pa. The software used is GEMINI (Thermodata).[12] The calculations were carried out under isobar and isothermal conditions. Indeed, the pressure and the temperature will be maintained constant during the experimental tests.

SiC-based ceramics follow two types of oxidation, passive and active, depending on the oxygen partial pressure and temperature. The passive oxidation leads to formation of a silica protective layer which slows down further oxidation. The passive oxidation reaction of SiC with oxygen at high temperature is described by:

$$SiC(s) + 3/2O_2(g) = SiO_2(s) + CO(g)$$

The active oxidation leads to the formation of volatile oxides SiO(g) and CO(g), and consequently, a mass loss of SiC is observed according to the reaction:

$$SiC(s) + O_2(g) = SiO(g) + CO(g)$$

At the passive/active transition, there are 6 species present: He(g), O_2(g), SiC(s), SiO_2(s), CO(g) and SiO(g). These species are connected by two chemical equilibriums and can exist in the form of three phases: two solid phases SiC(s) and SiO_2(s) and a gaseous one. The variance of the system is 3, hence, an additional parameter has to be taken into account to define the system at the thermodynamic equilibrium, in addition to the total pressure P^t and temperature T, it is the oxygen partial pressure. Indeed, experimentally, the three parameters that can be controlled are the temperature, the total pressure inside the chamber of the reactor and the oxygen partial pressure of the carrier gas.

Fig. 1 shows the variation of the number of moles of solid species versus temperature for the oxidation of β-SiC in an

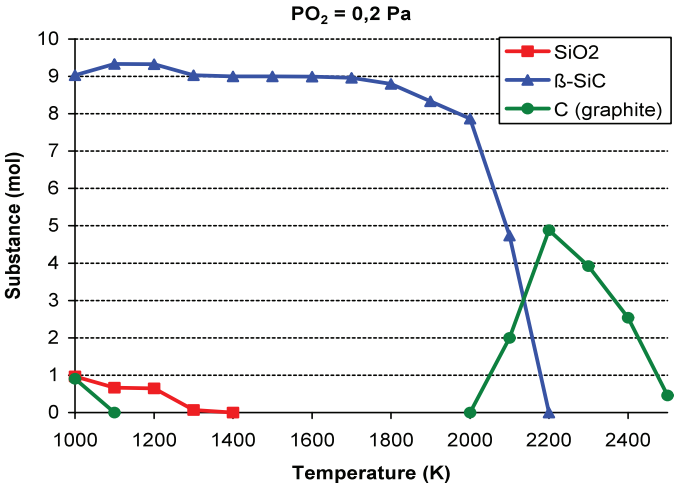

Fig. 1. Variation of the number of moles of solid species versus temperature under $pO_2 = 0.2$ Pa.

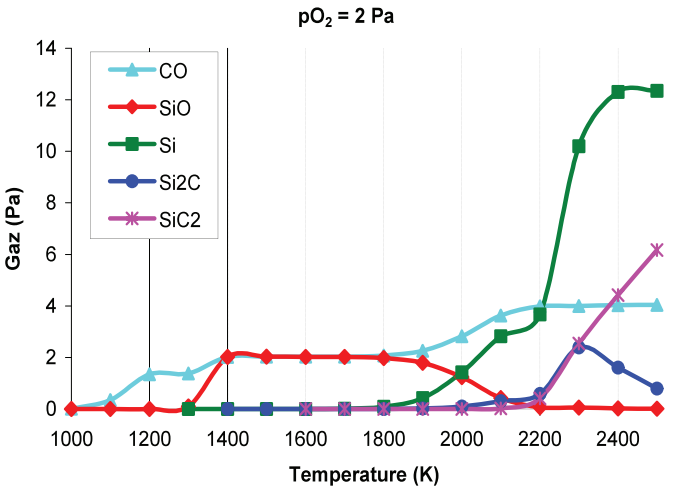

Fig. 3. Variation of partial pressures of gases produced versus temperature under $pO_2 = 2$ Pa.

atmosphere containing 0.2 Pa of oxygen. Fig. 2 shows the partial pressures of the gases produced versus temperature for the same oxygen partial pressure. It can be seen in Fig. 1 that silica is thermodynamically not stable above 1300 K, and that from this temperature we observe in Fig. 2 a stable period (plateau) for the equilibrium partial pressures: $p^e(CO) = p^e(SiO) \sim 0.2$ Pa on the range 1300–1600 K. Beyond 1600 K, the SiO partial pressure decreases (and that of CO increases) and the species Si, Si_2C and SiC_2 appear due to the sublimation of SiC at high temperature. Based on these observations, we define the passive/active transition temperature, T^{p-a}, as the temperature at which $p^e(SiO)$ reaches the stable period such as $p^e(SiO) = p^e(CO)$.

The same calculations were carried out for oxygen partial pressures equal to 2, 10, 30, 60 and 100 Pa. These calculations show that a higher oxygen partial pressure stabilizes the silica at higher temperatures, and the number of moles of SiC consumed by sublimation is lower. Therefore, we expect a shift towards higher temperatures for the passive/active transition. Fig. 3 shows, for example, the calculations obtained for $pO_2 = 2$ Pa.

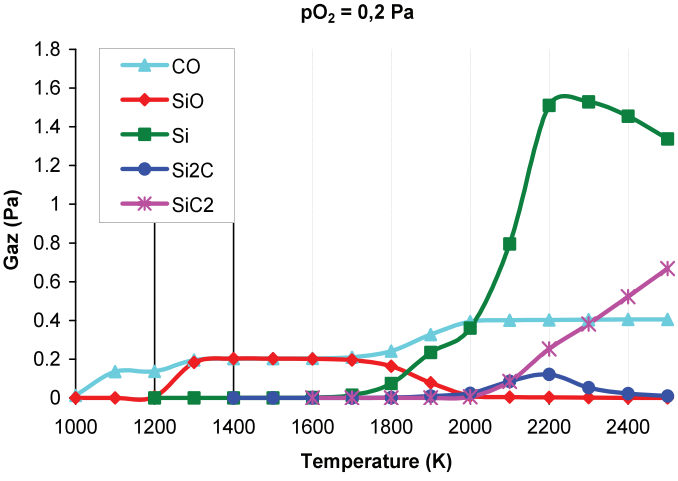

Fig. 2. Variation of partial pressures of gases produced versus temperature under $pO_2 = 0.2$ Pa.

In this figure, we see an increase of the passive/active transition temperature T^{p-a} of nearly 100 K and also of the SiC sublimation temperature. The calculations indicate a passive/active transition temperature T^{p-a} equal to 1300 K and 1400 K, respectively, under pO_2 equal to 0.2 and 2 Pa.

3. Experimental study

This study focuses on the oxidation behavior of β-SiC–SiC/PyC/SiC composite in low oxygen partial pressure in helium atmosphere, in the temperature range of nominal operation conditions of the GFR and in the case of accident and, on the degradation kinetics in accidental conditions. The oxidation tests were performed using the high pressure and temperature solar reactor (REHPTS) facility formerly described.[10] This reactor installed at the focus of the 5 kW solar furnace allows studying the behavior of materials subjected to high temperatures under controlled atmosphere with increase temperature speed ranging from 10 to 100 K/s similar to those that may occur during an incident or accident in a nuclear reactor.

3.1. Material and oxidation protocol

The oxidation tests were conducted on a β-SiC–SiC/PyC/SiC composite developed by Snecma Propulsion Solide (SPS), France. This material consists of a β-SiC matrix produced by CVI (chemical vapor infiltration) and reinforced by Hi-Nicalon fibers (β-SiC) with a pyrocarbon interphase (PyC). A β-SiC coating deposited by the CVD (chemical vapor deposition) method on one face is used to close the porosity of the surface.

To reproduce the possible atmospheres of the GFR, different helium qualities from Air Liquide were used: He Alphagaz1 with 2 ppm O_2 and 1 ppm H_2O and He U with 20 ppm O_2, with a gas flow of 10 l/min. Samples were oxidized during 10 min at constant temperatures ranging from 1400 to 2300 K. The heating rate up to the plateau is between 20 and 100 K/s and the cooling

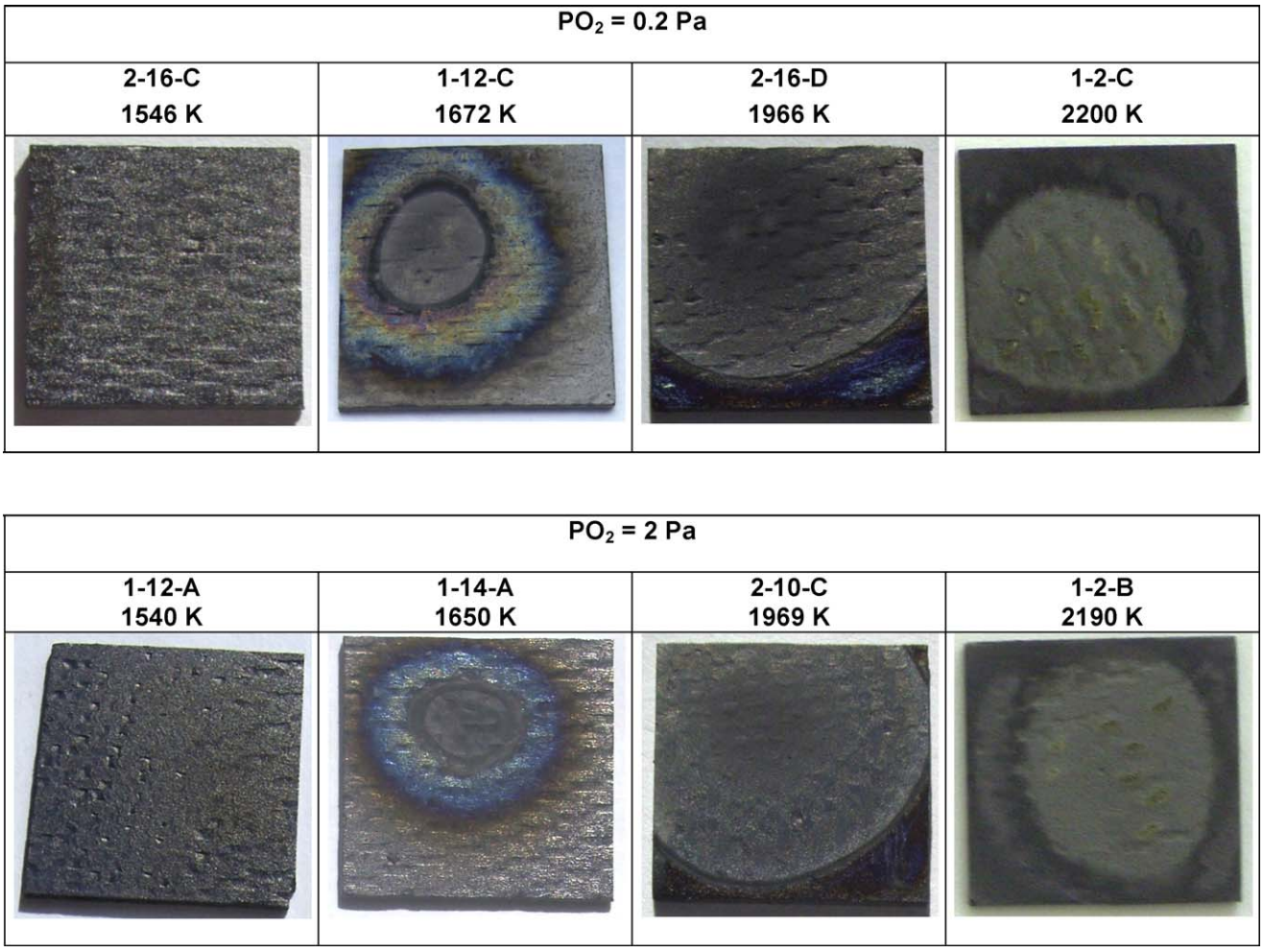

Fig. 4. Photos of β-SiC–SiC/PyC/SiC composites after oxidation under $pO_2 = 0.2$ and 2 Pa at different temperatures.

down to the room temperature is about 20 K/s. The total pressure inside the REHPTS is maintained at 10^5 Pa.

The samples are weighed before and after oxidation in order to calculate the relative mass changes (average value). SEM imaging was performed to analyze the surface morphology.

Some samples were pre-oxidized during 48 h at 1300 K under air inside an electrical furnace to develop a silica layer before being treated inside the REHPTS under helium with $pO_2 = 2$ Pa, in order to define the effect of a silica layer on the active oxidation kinetics.

3.2. Results and discussion

3.2.1. Oxidation experiments and surface characterization

Tables 1 and 2 summarize the experimental conditions of the various tests carried out on β-SiC–SiC/PyC/SiC composite under $pO_2 = 0.2$ and 2 Pa, and the corresponding mass variations, given in percentage and in mg cm^{-2} min^{-1}.

Fig. 4 presents the photographs of some representative samples of β-SiC–SiC/PyC/SiC oxidized under $pO_2 = 0.2$ and 2 Pa. The images of Fig. 4 present different zones due to the thermal gradient on the surface during heating by concentrated solar radiation.[10] For temperatures from 1540 K to 1670 K, the shutter is not fully open to reach these temperature levels so the solar flux distribution is not the same as for images around 2200 K with a nearly fully opening of the shutter. The temperature measurement is always performed in the center of the sample on a 6 mm diameter circle.[10] Thus, we notice three different surface morphologies according to the oxidation temperature:

Table 1
Summary of the tests carried out on β-SiC–SiC/PyC/SiC composite oxidized under $pO_2 = 0.2$ Pa, temperature conditions, oxidation regime identified and mass change rate.

$pO_2 = 0.2$ Pa				
Sample reference	T (K)	Oxidation regime	$\Delta m/m_0$ (%)	Mass change rate (mg cm^{-2} min^{-1})
2-16-C	1546	Passive	0.06	0.02
1-12-C	1672	Passive/Active	0.00	0.00
2-16-A	1855	Active	−0.15	−0.04
2-16-D	1966	Active	−0.51	−0.14
6-14-C	2024	Active	−0.85	−0.23
1-1-B	2073	Active	−1.33	−0.36
1-1-C	2100	Active	−2.47	−0.68
2-16-B	2126	Active	−2.72	−0.78
1-2-C	2200	Active	−5.15	−1.33

Table 2
Summary of the tests carried out on β-SiC–SiC/PyC/SiC composite oxidized under $pO_2 = 2$ Pa, temperature conditions, oxidation regime identified and mass change rate.

$pO_2 = 2$ Pa				
Sample reference	T (K)	Oxidation regime	$\Delta m/m_0$ (%)	Mass change rate (mg cm^{-2} min^{-1})
1-12-A	1540	Passive	−0.03	−0.01
1-14-A	1650	Passive/Active	−0.12	−0.03
1-14-B	1740	Active	−0.22	−0.06
2-10-C	1969	Active	−0.35	−0.09
6-14-B	2036	Active	−0.85	−0.23
6-14-A	2100	Active	−1.41	−0.39
1-14-C	2160	Active	−1.63	−0.44
1-2-B	2190	Active	−4.54	−1.10
1-1-A	2203	Active	−4.87	−1.59
2-10-D	2215	Active	−2.86	−0.69
1-1-D	2250	Active	−7.70	−2.06

(1) a representative surface for passive oxidation (samples oxidized at 1546 and 1540 K) looking like the virgin samples, (2) a surface presenting a limit state between passive oxidation and active oxidation (samples oxidized at 1672 and 1650 K) and (3) a more damaged surface representative of active oxidation (samples oxidized at 1966, 2200, 1969 and 2190 K). In this last case, we note the existence on the samples oxidized at very high temperature, $T > 2100$ K under $pO_2 = 0.2$ Pa and $T > 2160$ K under $pO_2 = 2$ Pa, of greenish zones representative of areas more attacked than the rest of the sample (samples oxidized at 2200 and 2190 K).

Fig. 5 shows the SEM images and the oxidation regime of characteristic samples of β-SiC–SiC/PyC/SiC oxidized under $pO_2 = 2$ Pa. We can see in the image: (a) the surface of the reference sample, (b) the presence of a silica layer characteristic of passive oxidation, (c) a limit state between passive (silica crystals and needles appearing as white) oxidation and active (grey parts with a lot of holes) oxidation and for the other samples, (d), (e) and (f), the presence of a surface increasingly attacked which is characteristic of active oxidation. It may be noticed that in the case of active oxidation, various surface states are observed according to the temperature level. Indeed, for samples oxidized under active oxidation conditions at 'moderate' temperatures – sample (d) – the surface appears covered with small grains and rather rough, while for samples oxidized at higher temperatures – sample (f) – the surface appears with large

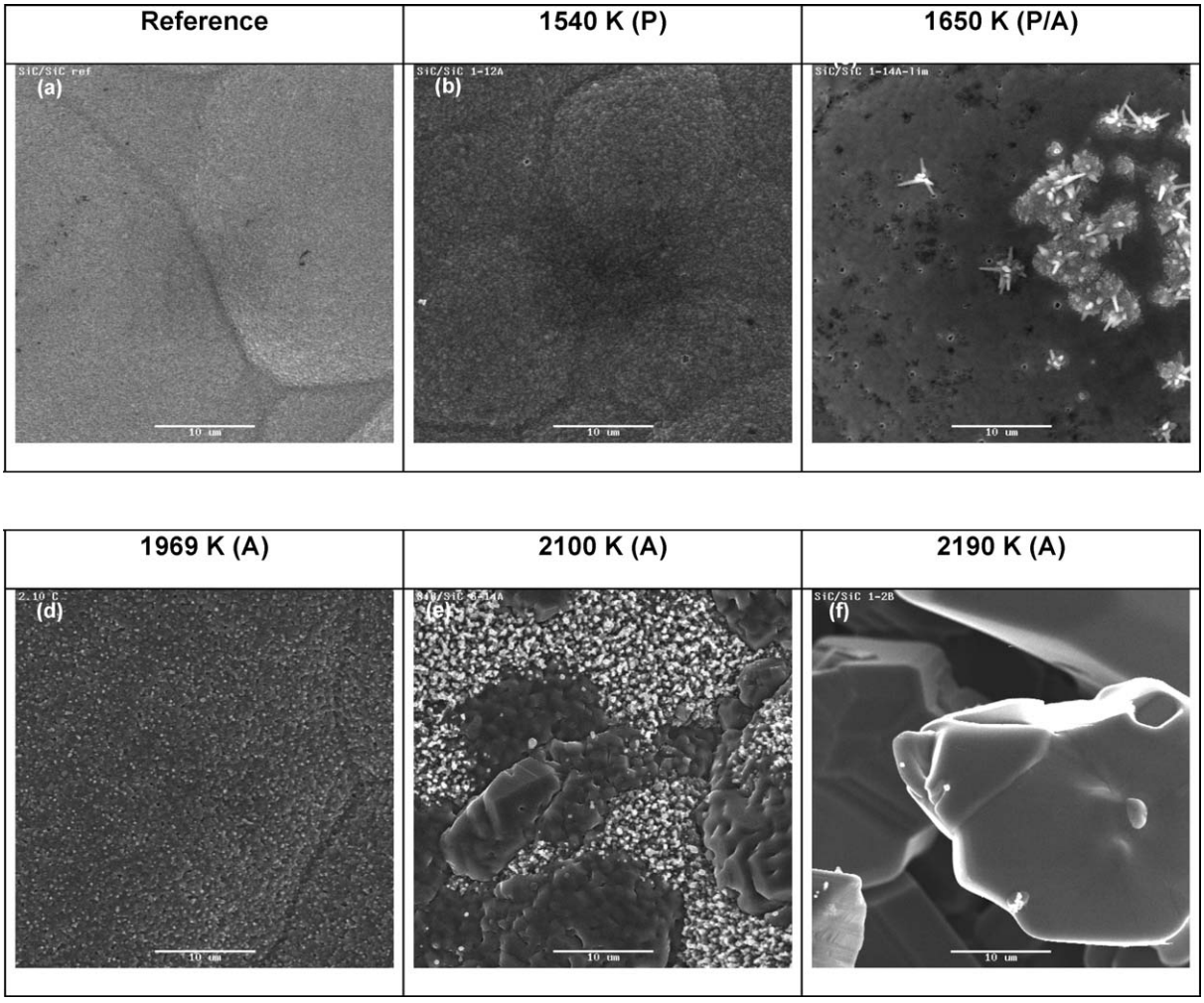

Fig. 5. SEM images of the surface of β-SiC–SiC/PyC/SiC composites before (a) and after oxidation under $pO_2 = 2$ Pa at 1540 K (b), 1650 K (c), 1969 K (d), 2100 K (e) and 2190 K (f).

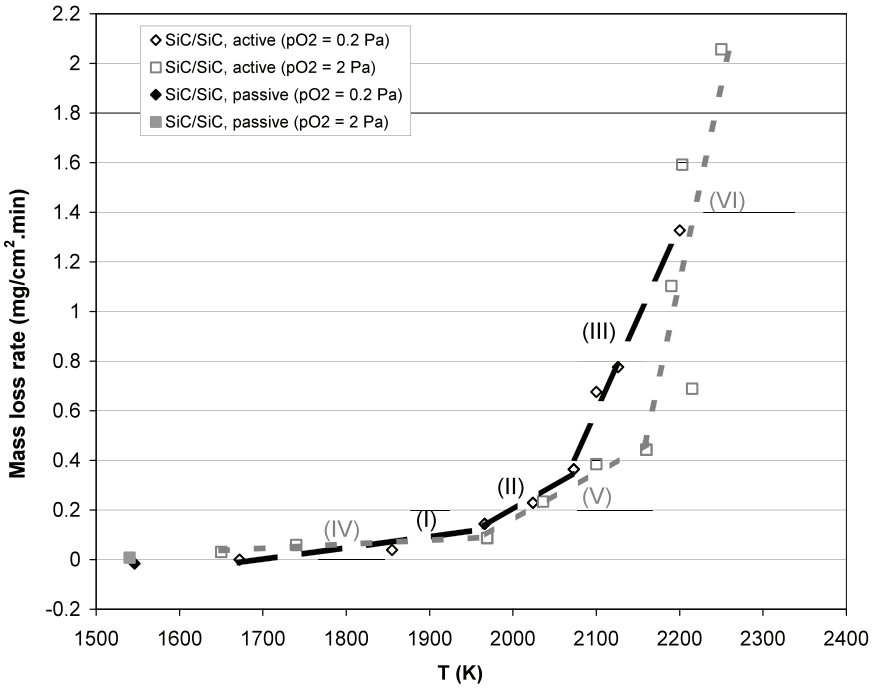

Fig. 6. Comparison between the mass loss rates according to temperature for β-SiC–SiC/PyC/SiC (simply labeled in the graph SiC/SiC) oxidized under $pO_2 = 0.2$ and 2 Pa.

smooth grains surrounded by several large porosities. We note that a limit case between these two ones is observed on the sample (e). The same observations were noticed in the case of $pO_2 = 0.2$ Pa.

We can see that by increasing the temperature, the surface appears more attacked with a larger porosity emerging on the surface. The replacement of small grains by larger grains is observed from 2070 K under $pO_2 = 0.2$ Pa and from 2100 K under $pO_2 = 2$ Pa. This replacement may be related to the coalescence of some grains at high temperature coupled with the consumption of small grains by sublimation. In fact, according to the thermodynamic calculation that have been performed on the oxidation of SiC in the same conditions as in the experimental tests, $pO_2 = 0.2$ and 2 Pa (Figs. 2 and 3), it appears that for temperatures between 1400 and 2000 K, an active oxidation takes place leading to formation of SiO(g) and CO(g) on the sample surface, this resulting in the production of small grains due to the recession of the original ones. For temperatures above 2000 K, the predominant species given by the thermodynamic calculation are in this case: Si(g), Si_2C(g) and SiC_2(g), due to the sublimation of SiC(s) at very high temperatures. Compared to the microstructure, we note that the sublimation of SiC leads to the disappearance of the small grains of the surface and some grains become replaced by large ones (coalescence) with larger porosities observed.

3.2.2. Kinetics of active oxidation

Fig. 6 shows the evolution of the mass loss rate versus temperature for β-SiC–SiC/PyC/SiC oxidized under $pO_2 = 0.2$ and 2 Pa. These variations are calculated in mg cm^{-2} min^{-1} taking into account the total surface of the sample (front face submitted to the concentrated solar radiation), they are average values obtained after a 10 min heat treatment on a temperature plateau, this being more detailed in Ref. 10. We note that the variation of the mass loss rate as a percentage – $\Delta m/m_0$ (%) – versus temperature shows the same trend line appearance as those obtained for the mass loss rate expressed in mg cm^{-2} min^{-1}.

In addition, this representation gives a clear vision of the impact of temperature on the mass loss rate. Thus, we notice the existence of three domains in the active oxidation regime for the two oxygen partial pressures. In the case of $pO_2 = 0.2$ Pa, we observe a linear and low mass loss rate up to 1970 K, domain (I), then a significant increase of the mass loss rate in two steps, domains (II) and (III). The domain (II) shows a mass loss rate increasing 4 times higher than that of the domain (I), whereas, the domain (III) shows a 3.6 times increase more important than that of the domain (II). The equations of linear trends are the following ones with the corresponding correlation coefficient (v in mg cm^{-2} min^{-1} and T in K):

$$\begin{aligned}
&\text{domain (I)} && 1670 \le T \le 1970\,\text{K} && v = 0.0005T - 0.79 && (R^2 = 0.85)\\
&\text{domain (II)} && 1970 \le T \le 2070\,\text{K} && v = 0.0020T - 3.88 && (R^2 = 0.97)\\
&\text{domain (III)} && 2070 \le T \le 2200\,\text{K} && v = 0.0073T - 14.71 && (R^2 = 0.98)
\end{aligned}$$

In the case of $pO_2 = 2$ Pa, we note again the existence of three domains in the active oxidation regime. The corresponding

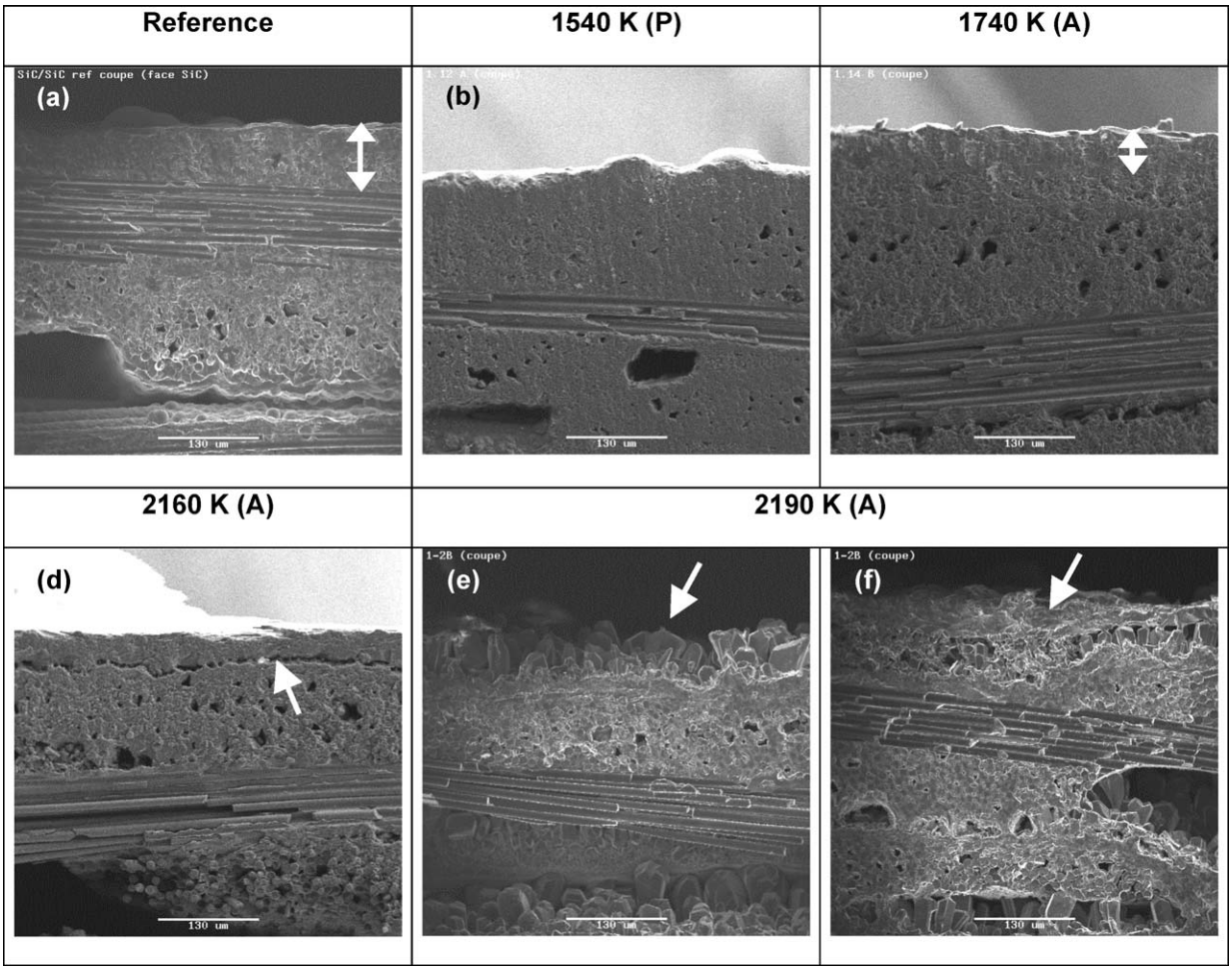

Fig. 7. SEM images of transverse cross-sections of β-SiC–SiC/PyC/SiC before (a) and after oxidation under $pO_2 = 2$ Pa at 1540 K (b), 1740 K (c), 2160 K (d) and at 2190 K (observation in the level of a greenish zone (e) and of a grey zone (f)).

linear trends are the following ones with the corresponding correlation coefficient (v in mg cm^{-2} min^{-1} and T in K):

domain (IV)	$1650 \leq T \leq 1970$ K	$v = 0.0002T - 0.24$	$(R^2 = 0.94)$
domain (V)	$1970 \leq T \leq 2160$ K	$v = 0.0019T - 3.68$	$(R^2 = 0.97)$
domain (VI)	$2160 \leq T \leq 2250$ K	$v = 0.0156T - 33.14$	$(R^2 = 0.61)$

In this case, the increase of the mass loss rate is more important than the one calculated under $pO_2 = 0.2$ Pa. Thus, the mass loss rate of the domain (V) is 9.5 times more important than that of the domain (IV) and the mass loss rate of the domain (VI) is 8 times more important than that of the domain (V) (compared, respectively, to 4 and 3.6 times more important under $pO_2 = 0.2$ Pa).

To explain the first increase of the mass loss rate (domains II and V), we refer to the observations of the transverse cross-sections which were carried out on some representative samples of the domain (V) oxidized under $pO_2 = 2$ Pa, e.g. the sample oxidized at 2160 K, Fig. 7(d). Indeed, the SEM micrographs reveal a surface matrix detached from the body of the composite with a more important degradation of the β-SiC coating compared to a non-oxidized matrix and β-SiC coating observed in the case of the reference sample (Fig. 7(a)) and in the case of the domain (IV) samples (e.g. samples oxidized at 1540 and 1740 K, Fig. 7(b) and (c)). Thus, the body of the composite is more and more exposed to the oxidizing atmosphere and a very damaging oxidation is taking place which is characterized by an increase of the mass loss rate. Same observations were noticed in the case of the samples oxidized under $pO_2 = 0.2$ Pa.

Above 2160 K for $pO_2 = 2$ Pa and 2070 K for $pO_2 = 0.2$ Pa, the β-SiC–SiC/PyC/SiC composite shows a huge increase of the mass loss rate. Indeed, it appears that the sublimation of SiC(s) to Si(g), Si_2C(g) and SiC_2(g) starts at this temperature leading to an important mass loss rate. This is in agreement with the thermodynamic calculations that were performed on the oxidation of β-SiC in the same conditions as in the experimental tests ($pO_2 = 0.2$ and 2 Pa) (Figs. 2 and 3).

Table 3
Summary of the tests carried out on the uncoated face of SiC/PyC/SiC composite under $pO_2 = 2$ Pa, temperature conditions and mass change rate.

$pO_2 = 2$ Pa; uncoated face			
Sample reference	T (K)	$\Delta m/m_0$ (%)	Mass change rate (mg cm^{-2} min^{-1})
7-3-B	1762	−0.12	−0.04
1-2-D	1973	−0.78	−0.20
6-12-A	2130	−1.53	−0.42
7-3-D	2177	−2.26	−0.61
6-14-D	2205	−2.27	−0.61
7-3-A	2224	−3.71	−1.03

Table 4
Summary of the tests carried out on pre-oxidized SiO_2-β-SiC–SiC/PyC/SiC composites under $pO_2 = 2$ Pa, temperature conditions and mass change rate.

$pO_2 = 2$ Pa; samples pre-oxidized during 48 h under air at 1300 K			
Sample reference	T (K)	$\Delta m/m_0$ (%)	Mass change rate (mg cm^{-2} min^{-1})
6-8-C	1760	−0.14	−0.04
6-8-D	1887	−0.28	−0.08
6-8-A	2165	−3.36	−0.91
2-10-A	2170	−1.69	−0.38
2-10-B	2208	−3.92	−0.72

This sublimation reaction explains the greenish zones observed on the surface of the samples exposed to very high temperatures (Fig. 4, samples 1-2-C and 1-2-B). Indeed, the SEM observations of transverse cross-sections carried out on these zones show that the β-SiC coating has nearly completely disappeared along with an advanced oxidation of the matrix (Fig. 7(e) and (f)). This advanced degradation, preferentially on some zones of the surface, can be explained by a SiC layer (matrix + coating) more or less thick according to irregular surface roughness of the composite. A longer exposure under these conditions will lead to a total revealing of the body of the composite. In addition, the chemical analyses performed by EDS in these greenish zones and grey areas around them showed, in both cases, a typical composition of SiC.

These results show, for temperatures lower than 2070 K, the weak impact of oxygen partial pressure (in the range 0.2–2 Pa) on the mass loss rate of material. For both operative pressures and beyond 2070 K, the composite β-SiC–SiC/PyC/SiC shows an increase in the degradation rate. This increase occurs at a lower temperature for $pO_2 = 0.2$ Pa than for $pO_2 = 2$ Pa. This difference could be associated with the increase of the SiC sublimation temperature according to pO_2 as shown by the thermodynamic calculations (Figs. 2 and 3).

3.2.3. Oxidation study on the uncoated face

In order to study the role of the β-SiC coating, some oxidation tests were also performed under incidental and accidental operating conditions on the SiC/PyC/SiC samples on the uncoated face. Table 3 summarizes the various tests conducted under $pO_2 = 2$ Pa.

By comparison to the SEM observations of the oxidized samples, we notice the same surface morphology as that observed in the case of the samples oxidized on the coated face.

Fig. 8 shows the evolution of the mass loss rates versus temperature for the SiC/PyC/SiC oxidized under $pO_2 = 2$ Pa. The empty circles represent the results obtained on the uncoated face. Thus, we note in this case, the existence of two oxidation domains in the zone of active oxidation. The equations of linear trends are the following ones with the corresponding correlation coefficient (v in mg cm^{-2} min^{-1} and T in K):

$$\text{domain (VII)} \quad 1760 \le T \le 2170\ \text{K} \quad v = 0.0013T - 2.28 \quad (R^2 = 0.92)$$

$$\text{domain (VIII)} \quad 2170 \le T \le 2220\ \text{K} \quad v = 0.0083T - 17.58 \quad (R^2 = 0.65)$$

Compared to the results obtained on the samples oxidized on the coated face, the results obtained on the uncoated face are very close with linear mass loss rate between 1760 and 2170 K which strongly increases beyond 2170 K due to the sublimation of SiC at very high temperature. This last point is the most important one showing that the coating is not very useful in case of accidental conditions.

The mass loss rates and the SEM observations do not show a great influence of the β-SiC coating on the oxidation behavior of β-SiC–SiC/PyC/SiC at high temperature. This coating which seems to be too thin (as shown by the SEM observations of transverse cross-sections) in case of accidental conditions of the GFR (active oxidation) to show a remarkable effect on the oxidation rate, remains essential to close the porosity of the surface and to prevent a direct contact between the reactant gases and the body of the composite. This can explain the linear trend of the mass loss rate between 1760 and 2170 K obtained on SiC/PyC/SiC oxidized on the uncoated face due to direct internal oxidation of the body of the composite, compared to the mass loss rate observed on β-SiC–SiC/PyC/SiC oxidized on the coated face. Nevertheless, to be sure of the trend followed for the uncoated face of the sample, more experiments have to be performed.

3.2.4. Study on pre-oxidized samples

Table 4 summarizes the experimental conditions for tests carried out on SiO_2-β-SiC–SiC/PyC/SiC pre-oxidized during 48 h under air at 1300 K, and the corresponding mass variations, given in percentage and in mg cm^{-2} min^{-1}. The SEM observations of the oxidized samples show again and according to temperature, a change in the surface morphology from a surface covered with small grains to a smooth surface composed of large grains. This change occurs at temperatures around 2170 K like in the case of the non-pre-oxidized samples.

The solid squares on Fig. 8 represent the tests carried out on the pre-oxidized samples. The equations of linear trends which take into account these points together with the ones obtained on non pre-oxidized samples (coated face) are the

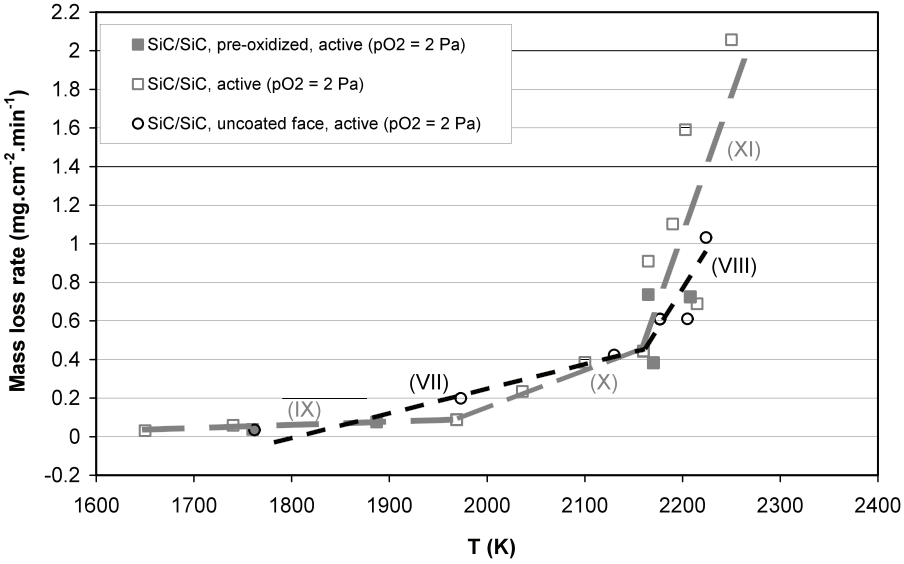

Fig. 8. Evolution of the mass loss rate versus temperature for β-SiC–SiC/PyC/SiC (simply labeled in the graph SiC/SiC) oxidized under $pO_2 = 2$ Pa. The empty circles represent the tests performed on SiC/PyC/SiC composite oxidized from the uncoated face and the solid squares represent the tests performed on the pre-oxidized SiO_2-β-SiC–SiC/PyC/SiC samples.

following ones with the corresponding correlation coefficient (v in mg cm^{-2} min^{-1} and T in K):

domain (IX)	$1650 \leq T \leq 1970$ K	$v = 0.0002T - 0.24$	$(R^2 = 0.94)$
domain (X)	$1970 \leq T \leq 2160$ K	$v = 0.0016T - 3.07$	$(R^2 = 0.90)$
domain (XI)	$2160 \leq T \leq 2250$ K	$v = 0.0140T - 29.80$	$(R^2 = 0.54)$

It can be seen, by comparison between the results obtained on pre-oxidized samples with those on normal samples, that the presence of a silica layer on the surface, formed after pre-oxidation under air during 48 h, does not affect the kinetics of active oxidation in accidental conditions. For the GFR, it is clear that the formation of SiO_2 during the nominal operation mode is stabilized after a certain duration. The silica layer thus formed remains in all cases very thin and volatilizes very quickly in the case of an accident at high temperature and consequently does not protect the material from aggravated active oxidation.

4. Conclusion

The experimental study carried out on the β-SiC–SiC/PyC/SiC composites has allowed to determine the oxidation rates under incidental and accidental operating conditions for two low oxygen partial pressures, 0.2 and 2 Pa, for a total pressure of 10^5 Pa (helium). In fact, the evolution of the mass loss rates versus temperature for β-SiC–SiC/PyC/SiC oxidized under $pO_2 = 0.2$ and 2 Pa shows the existence of three domains in the active oxidation regime. These experiments have also shown the weak impact of oxygen partial pressure on the mass loss rate, in the range 0.2–2 Pa, for temperatures below 2070 K. However, beyond 2070 K, we notice an increase of the mass loss rate at lower temperatures for $pO_2 = 0.2$ Pa than for $pO_2 = 2$ Pa. This difference was associated to the effect of the oxygen partial pressure on the sublimation temperature of SiC as given by the thermodynamic calculation.

For the tests carried out on SiC/PyC/SiC on the uncoated face, the results do not show a great influence of the β-SiC coating on the oxidation behavior at very high temperature (active oxidation). This coating which seems to be too thin to show a remarkable effect on the oxidation rate remains essential to close the surface porosity and to prevent a direct contact between the reactant gases and the body of the composite.

In the case of the pre-oxidized samples, the variation of mass loss rate and the SEM observations do not show a great importance of SiO_2 layer formed after pre-oxidation. This layer will not protect the β-SiC–SiC/PyC/SiC in accidental operating conditions.

Acknowledgements

The authors thank the research group GDR MATINEX for its support and the CEA for funding the post-doctoral position of K. Dawi.

References

1. Katoh Y, Snead LL, Henager Jr CH, Hasagawa A, Kohyama A, Riccardi B, et al. Current status and critical issues for development of SiC composites for fusion applications. *J Nucl Mater* 2007;**367–370**:659–71.
2. Nogami S, Otake N, Hasegawa A, Katoh Y, Yoshikawa A, Satou M, et al. Oxidation behavior of SiC/SiC composite for helium cooled solid breeder blanket. *Fusion Eng Des* 2008;**83**:1490–4.

3. Filipuzzi L, Camus G, Naslain R, Thébault J. Oxidation mechanisms and kinetics of 1D-SiC/C/SiC composite materials: I. An experimental approach. *J Am Ceram Soc* 1994;**77**:459–66.
4. Wu S, Cheng L, Zhang L, Xu Y, Zhang Q. Comparison of oxidation behaviors of 3D C/PyC/SiC and SiC/PyC/SiC composites in an O_2-Ar atmosphere. *Mater Sci Eng B* 2006;**130**:215–9.
5. Wu S, Cheng L, Zhang L, Xu Y, Zhang Q. Oxidation behavior of 3D Hi-Nicalon/SiC composite. *Mater Lett* 2006;**60**:3197–201.
6. Ochiai S, Kimura S, Tanaka H, Tanaka M, Hojo M, Morishita K, et al. Residual strength of PIP-processed SiC/SiC single-tow minicomposite exposed at high temperatures in air as a function of exposure temperature and time. *Composites Part A* 2004;**35**:41–50.
7. Ochiai S, Kimura S, Tanaka H, Tanaka M, Hojo M, Morishita K, et al. Degradation of SiC/SiC composite due to exposure at high temperatures in vacuum in comparison with that in air. *Composites Part A* 2004;**35**:33–40.
8. Balat MJH. Determination of the active-to-passive transition in the oxidation of silicon carbide in standard and microwave-excited air. *J Eur Ceram Soc* 1996;**16**:55–62.
9. Lamouroux F, Camus G, Thébault J. Kinetics and mechanisms of oxidation of 2D woven composites C/SiC composites: I. Experimental approach. *J Am Ceram Soc* 1994;**77**:2049–57.
10. Charpentier L, Balat-Pichelin M, Audubert F. High temperature oxidation of SiC under helium with low-pressure oxygen – Part 1: Sintered α-SiC. *J Eur Ceram Soc* 2010;**30**:2653–60.
11. Charpentier L, Balat-Pichelin M, Glénat H, Bêche E, Laborde E, Audubert F. High temperature oxidation of SiC under helium with low-pressure oxygen – Part 2: CVD β-SiC. *J Eur Ceram Soc* 2010;**30**:2661–70.
12. Thermodata, 38400 Saint Martin d'Hères, France.